Communications in Mathematics and Applications
Vol. 14, No. 5, pp. 1857–1870, 2023
ISSN 0975-8607 (online); 0976-5905 (print)
Published by RGN Publications
DOI: 10.26713/cma.v14i5.2203

http://www.rgnpublications.com

Research Article

Effects of Non-Uniform Heat Source-Sink and Nonlinear Thermal Radiation on MHD Heat and Mass Transfer in a Thin Liquid Film

Prasenjit Saha

Department of Mathematics, Suri Vidyasagar College, Suri, Birbhum 731 101, West Bengal, India
sahaprasenjit123@gmail.com

Received: February 3, 2023 **Accepted:** May 21, 2023

Abstract. This paper describes the non-uniform heat source/sink effect on MHD heat and mass transfer of a thin liquid film taking nonlinear thermal radiation over a permeable unsteady stretching surface. Boundary conditions are taken as convective type. Similarity transformation are used to convert unsteady boundary layer equations to a system of non-linear ordinary differential equations. For the presence of nonlinear thermal radiation term in the energy equation the momentum, energy and mass-diffusion equations are highly non-linear. Thus, we can not be solved the problem analytically. To solve the problem we use numerical Runge-Kutta-Fehlberg method with shooting technique. Shooting technique helps us to determine the unknown initial condition. The effect of various parameters like Prandtl number, Schmidth number, source/sink parameters, radiation parameters, magnetic parameter, unsteadiness parameter are shown and discuss here. Some numerical results are compare in a table with previous work. It is found that increase in space dependent heat source/sink parameter and temperature dependent heat source/sink parameter decreases temperature gradient. Thermal radiation decrease the cooling rate of the thin liquid film, also increase in magnetic parameter decreases velocity distribution and increase in the temperature and concentration gradients.

Keywords. Magnetohydrodynamic, Non uniform heat source-sink, Thin liquid film, Thermal radiation, Similarity transformation

Mathematics Subject Classification (2020). 76-10, 76A20, 76D05

1. Introduction

The study of heat and mass transfer in a thin liquid film has gained tremendous interest amongst researchers for the past few years for its industrial and engineering applications. The flow and heat transfer knowledge within a thin liquid film is used to understand the coating process and chemical processing equipments and design of various heat exchangers. The problem has scientific and engineering applications such as in extrusion process of metal and polymer, glass fiber and paper production, hot rolling, wire drawing, electronic chips, food processing, crystal growing, plastic manufactures and in application of paints. Such applications involve cooling of a molten liquid by drawing it into a cooling system. Sakiadis [11] initiated the study of the boundary layer flow generated by a continuous solid surface moving with a constant speed. Crane [4] studied the steady two-dimensional boundary layer flow of Newtonian fluids driven by the stretching plastic sheet. Wang [15] analyzed thin film flow over a horizontal stretching sheet using homotopy analysis method. Liu and Megahed [8] investigated effect of thermal radiation with variable heat flux in heat transfer aspect of a thin liquid film.

Khan *et al*. [5] analyzed numerical heat transfer and friction drag relating to Joule heating, viscous dissipation effect and heat generation/absorption in aligned MHD slip flow. Liu and Megahed [7] studied thin film flow and heat transfer over an unsteady stretching surface in presence of variable heat flux, thermal radiation and internal heating. Zhou *et al*. [16] investigated unsteady radiative slip flow of Casson fluid over a permeable stretched surface in presence of MHD and non-uniform heat source. Abel *et al*. [2] studied effect of non-uniform heat source on MHD heat transfer in a liquid film. Tsai *et al*. [13] investigate effects of non-uniform heat source on flow and heat transfer over an unsteady stretching surface. Aziz *et al*. [3] studied heat transfer in a liquid film taking permeable stretching sheet. Seddek and Salem [12] shows magnetic field effects on flow and heat transfer to a continuous moving flat plate. Vajravelu and Rollins [14] take magnetic field only to study heat transfer in an electrically conducting fluid over a stretching surface. Noor and Hashim [9] analyzed effects of magnetic field on the flow and heat transfer in a liquid film over an unsteady elastic stretching surface. Abel *et al*. [1] presents a mathematical analysis of flow and heat transfer to a laminar liquid film from a horizontal stretching surface in presence of magnetic field.

Motivated from the previous works, we consider in this paper the effects of non-uniform heat source/sink, non-linear thermal radiation on MHD heat and mass transfer in a thin liquid film over an unsteady stretching surface. The results obtained from the present work will provide useful information for application and also serve as a complement to the previous studies.

2. Formulation of the Problem

Let us consider a thin elastic sheet issues from a narrow slit at the origin of a Cartesian co-ordinate system. The continuous surface at $y=0$ is aligned with the x-axis and moves in its own plane (see Figure 1) with a velocity

$$U(x,t)=\frac{bx}{1-at}, \tag{1}$$

where b and a are both positive constant with dimension per time.

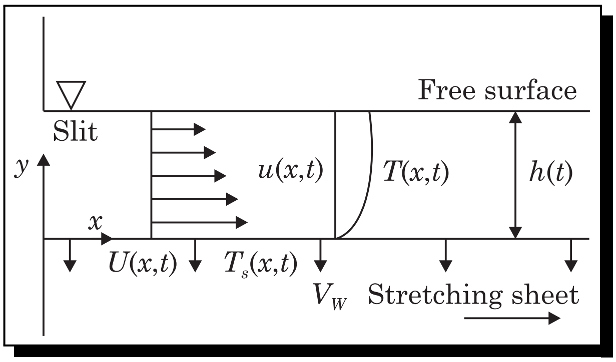

Figure 1. Geometrical configuration of the problem

The elastic sheet temperature T_s is assumed to vary both along the sheet and with time accordance with

$$T_s = T_0 - T_{ref}\left(\frac{dx^2}{\kappa\sqrt{\rho b/\mu}}\right)(1-at)^{-\frac{3}{2}}, \tag{2}$$

where T_0 is the temperature of the slit, T_{ref} is the constant reference temperature, ρ is the fluid density, t is time, μ is the viscosity of the fluid and κ be thermal conductivity of fluid.
The applied transverse magnetic field $B_1(t)$ is defined by Abel *et al*. [2]

$$B_1(t) = B_0(1-at)^{-\frac{1}{2}},$$

where B_0 is uniform magnetic field. A thin liquid film of uniform thickness $h(t)$ lies on the horizontal surface. The surface heat flux $q_t(x,t)$ at the stretching sheet varies with the power of distance x from the slit and with the inverse power of time factor t as [6]

$$q_t(x,t) = -\kappa\frac{\partial T}{\partial y} = -T_{ref}\frac{dx^2}{(1-at)^2}. \tag{3}$$

The surface mass flux $q_m(x,t)$ at the stretching sheet varies with the power of distance x from the slit and with the inverse power of time factor t as [13]

$$q_m(x,t) = -D\frac{\partial C}{\partial y} = -C_{ref}\frac{dx^2}{(1-at)^2}, \tag{4}$$

where κ is the thermal conductivity, T_{ref} is reference temperature, C_{ref} is reference concentration, d is a constant.
The boundary layer equations mass, momentum and for energy conservation are given by,

$$\frac{\partial u}{\partial x} + \frac{\partial v}{\partial y} = 0, \tag{5}$$

$$\frac{\partial u}{\partial t} + u\frac{\partial u}{\partial x} + v\frac{\partial u}{\partial y} = \frac{\mu}{\rho}\frac{\partial^2 u}{\partial y^2} - \frac{\sigma B_1^2}{\rho}u, \tag{6}$$

$$\frac{\partial T}{\partial t} + u\frac{\partial T}{\partial x} + v\frac{\partial T}{\partial y} = \frac{\kappa}{\rho C_p}\frac{\partial^2 T}{\partial y^2} - \frac{1}{\rho C_p}\frac{\partial q_r}{\partial y} + \frac{q'''}{\rho C_p}, \tag{7}$$

$$\frac{\partial C}{\partial t} + u\frac{\partial C}{\partial x} + v\frac{\partial C}{\partial y} = D\frac{\partial^2 C}{\partial y^2}, \tag{8}$$

where u and v are velocity components along the direction of x and y respectively. q_r called the radiative heat flux, C_p is the specific heat at constant pressure. The corresponding boundary conditions are:

$$\begin{cases} u = U(x,t),\ v = v_w,\ -k\dfrac{\partial T}{\partial y} = q_t(x,t),\ -D\dfrac{\partial C}{\partial y} = q_m(x,t) & \text{at } y = 0, \\ \dfrac{\partial u}{\partial y} = \dfrac{\partial T}{\partial y} = \dfrac{\partial C}{\partial y} = 0 & \text{at } y = h(t), \\ v = \dfrac{dh}{dt} & \text{at } y = h(t). \end{cases} \tag{9}$$

The non-uniform heat source/sink is modeled as

$$q''' = \frac{\kappa U}{x\nu}[A^*(T_s - T_0)f' + (T - T_0)B^*], \tag{10}$$

where A^* and B^* are the coefficients of space and temperature dependent heat source/sink respectively. Here, we make a note that the case $A^* > 0$, $B^* > 0$ corresponds to internal heat generation and that $A^* < 0$, $B^* < 0$ corresponds to internal heat absorption. $\nu = \frac{\mu}{\rho}$ is constant kinematic viscosity. The radiative heat flux q_r is taken according to Rosseland approximation as

$$q_r = -\frac{16\sigma^*}{3k^*}T^3\frac{\partial T}{\partial y}, \tag{11}$$

where σ^* is the Stefan-Boltzman constant, and k^* be the mean absorption coefficient.
The system of partial differential equations are transformed into a system of nonlinear ordinary differential equation by using the similarity transformations, which are given as follows:

$$\left.\begin{aligned} &\eta = \left(\frac{b}{\nu}\right)^{\frac{1}{2}}(1-at)^{-\frac{1}{2}}y, \\ &u = bx(1-at)^{-1}f'(\eta), \\ &v = -(b\nu)^{\frac{1}{2}}(1-at)^{-\frac{1}{2}}f(\eta), \\ &T = T_0 - T_{ref}\left(\frac{dx^2}{\kappa\sqrt{b/\nu}}\right)(1-at)^{-\frac{3}{2}}\theta(\eta), \\ &C = C_0 - C_{ref}\left(\frac{dx^2}{D\sqrt{b/\nu}}\right)(1-at)^{-\frac{3}{2}}\phi(\eta). \end{aligned}\right\} \tag{12}$$

The dimensionless thin film thickness β is defined by

$$\beta = \left(\frac{b}{\nu}\right)^{\frac{1}{2}}(1-at)^{-\frac{1}{2}}h(t). \tag{13}$$

The rate at which film thickness varies can be obtained by differentiating (13) with respect to t to obtain

$$\frac{dh}{dt} = -\frac{a\beta}{2}\left[\frac{\nu}{b(1-at)}\right]^{\frac{1}{2}}. \tag{14}$$

Thus, $v = \frac{dh}{dt}$ at $y = h(t)$ given by the boundary condition (9) which is transformed into the free surface condition (14).
The transformed set of ordinary differential equations are

$$f''' + \left(ff'' - f^2 - Sf' - \frac{S}{2}\eta f'' - Mf'\right) = 0, \tag{15}$$

$$\frac{1}{Pr}\theta'' + \frac{Nr}{Pr}(1+(\theta_w-1)\theta)^2[3(\theta_w-1)\theta'^2 + (1+(\theta_w-1)\theta)\theta'']$$
$$+\frac{1}{Pr}(A^*f' + B^*\theta) + \left[f\theta' - 2f'\theta - \frac{3}{2}S\theta - \frac{S}{2}\eta\theta'\right] = 0, \tag{16}$$

$$\phi'' - Sc\left[\frac{3S}{2}\phi + \frac{S}{2}\eta\phi' + 2f'\phi - f\phi'\right] = 0, \tag{17}$$

subject to the boundary conditions

$$\left.\begin{array}{l} f(0) = f_w,\ f'(0) = 1,\ \theta'(0) = -1,\ \phi'(0) = -1, \\ f''(\beta) = 0,\ \theta'(\beta) = 0,\ \phi'(\beta) = 0, \\ f(\beta) = \dfrac{S\beta}{2}, \end{array}\right\} \tag{18}$$

where prime represent differentiation with respect to η, $S = \frac{a}{b}$ be the unsteadiness parameter, $Pr = \frac{\mu c_p}{\kappa}$ be the Prandtl number, β be the dimensionless thin film thickness, $Nr = \frac{16\sigma^* T_0^3}{3k^*\kappa}$ be the radiation parameter, $\theta_w = \frac{T_s}{T_0}$ be the temperature ratio parameter, $Sc = \frac{\nu}{D}$ be the Schmidt number, $M = \frac{\sigma B_0^2}{\rho b}$ be the magnetic parameter, f_w being the permeability parameter.

3. Numerical Method

The non-linear differential eqs. (15), (16) and (17) with appropriate boundary conditions (18) are solved numerically by using Runge-Kutta-Fehlberg (RKF) fifth order technique along with shooting method. At a very first step, the higher order non-linear differential equations (15), (16) and (17) are converted into simultaneous differential equation of first order and further they are transformed into initial value problem by applying the shooting technique. Then initial value problem is solved by Runge-Kutta-Fehlberg fifth order method. The ordinary differential equations (15) to (17) which are of third order in f, second order in θ and second order in ϕ are reduced to a system of seven simultaneous equations of first order having seven unknowns. The convergence criterion is employed in the present work based on the difference between the value of the dependent variables of the present and previous iterations. When the absolute values of the difference reaches 10^{-6} which showed that the solution has converged to the desired accuracy then the iteration process is stopped. The governing non-linear ordinary differential equations are reduced to a set of simultaneous first order differential equation as follows:

$$y_1 = f,\ y_2 = f',\ y_3 = f'',\ y_4 = \theta,\ y_5 = \theta',\ y_6 = \phi,\ y_7 = \phi',$$

$$F_1 = y_2,\ F_2 = y_3,\ F_3 = -\left(y_1y_3 - y_2^2 - Sy_2 - \frac{S}{2}\eta y_3 - My_2\right),\ F_4 = y_5,$$

$$F_5 = \frac{-\left[3Nr(\theta_w-1)y_5^2(1+(\theta_w-1)y_4)^2 + (A^*y_2 + B^*y_4) + Pr(y_1y_5 - \frac{3}{2}Sy_4 - \frac{S}{2}\eta y_5 - 2y_2y_4)\right]}{[1+Nr(1+(\theta_w-1)y_4)^3]},$$

$$F_6 = y_7,\ F_7 = Sc\left(\frac{3S}{2}y_6 + \frac{S}{2}\eta y_7 + 2y_2y_6 - y_1y_7\right).$$

The boundary condition becomes

$$\begin{cases} y_1 = f_w,\ y_2 = 1,\ y_5 = -1,\ y_7 = -1, & \text{at } \eta = 0, \\ y_3 = 0,\ y_5 = 0,\ y_7 = 0, & \text{at } \eta = \beta. \end{cases}$$

Since the values of $y_3(0)$, $y_4(0)$, $y_6(0)$ are not prescribed, so we have to use the multiple shooting method to find three initial values. Then the resultant system of seven simultaneous equations is solved numerically by fifth-order Runge-Kutta-Fehlberg integration scheme (Saha [10]).

Table 1. Comparison of skin friction coefficient $-f''(0)$ and β values using RKF method when parameter $Nr = 0$, $M = 0$

	$-f''(0)$		β	
S	Liu and Megahed [10]	Present work	Liu and Megahed [10]	Present work
0.6	3.742316	3.742786	3.131252	3.1317100
0.8	2.680943	2.680962	2.151989	2.1519911
1.0	1.972317	1.972387	1.543622	1.5436177
1.2	1.442621	1.442627	1.127779	1.1277820
1.4	1.012735	1.012785	0.821033	0.8210349
1.6	0.642368	0.642402	0.576171	0.5761762
1.8	0.309134	0.309146	0.356390	0.3563941

4. Results and Discussion

The highly non-linear system of differential equations (15)-(17) subject to the boundary conditions (18) is solved numerically by using fifth order Runge-Kutta-Fehlberg numerical method with shooting technique. The effects of various important physical parameters such as heat source/sink parameter, magnetic parameter, Prandtl number Pr, thermal radiation parameter Nr, Schmidt number Sc and unsteadiness parameter S on non dimensional velocity components, temperature gradient, concentration gradient are analyzed and discussed in detail.

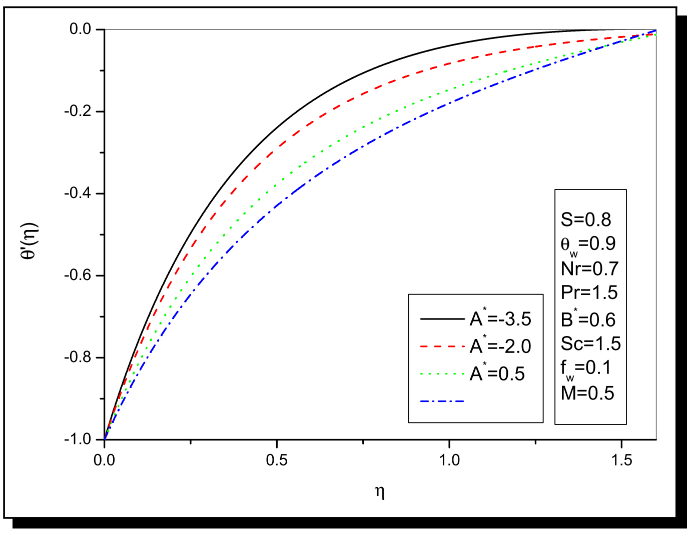

Figure 2. Effects of space dependent heat source/sink parameter A^* on temperature gradient $\theta'(\eta)$

Figure 2 shows the variation of temperature gradient for different values of space dependent heat source/sink parameter A^*. For increases of A^* temperature gradient is decreases.

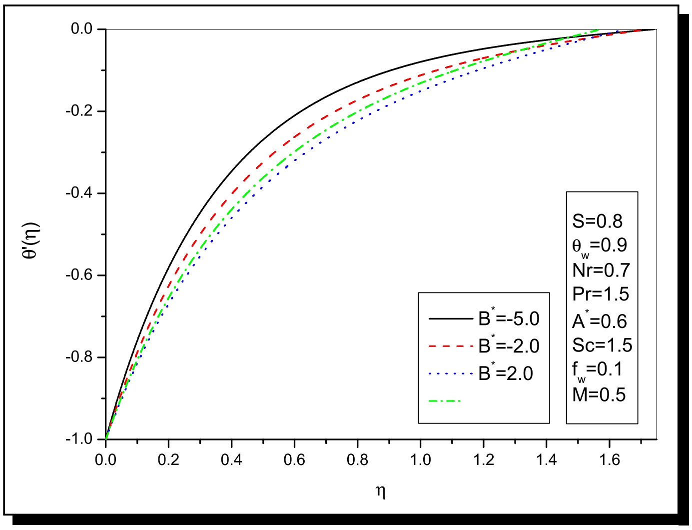

Figure 3. Effects of temperature dependent heat source/sink parameter B^* on temperature gradient $\theta'(\eta)$

Figure 3 shows the effect of temperature dependent heat source/sink parameter B^* on temperature gradient. For increases of B^* temperature gradient is decreases. We know the fact that the case $A^* > 0$, $B^* > 0$ correspond to internal heat generation and $A^* < 0$, $B^* < 0$ correspond to internal heat absorption. The heat generation/absorption depends on the axial flow f' and also on the boundary layer temperature T. The combine influence of the space dependent and temperature dependent heat source/sink parameters that determines the range of the temperature falls or rises in the boundary layer region. From these plots it is clear that the energy is released for increasing values of $A^* > 0$, $B^* > 0$ and therefore temperature gradient decrease, whereas energy is absorbed for decreasing values of $A^* < 0$, $B^* < 0$ resulting temperature gradient increase.

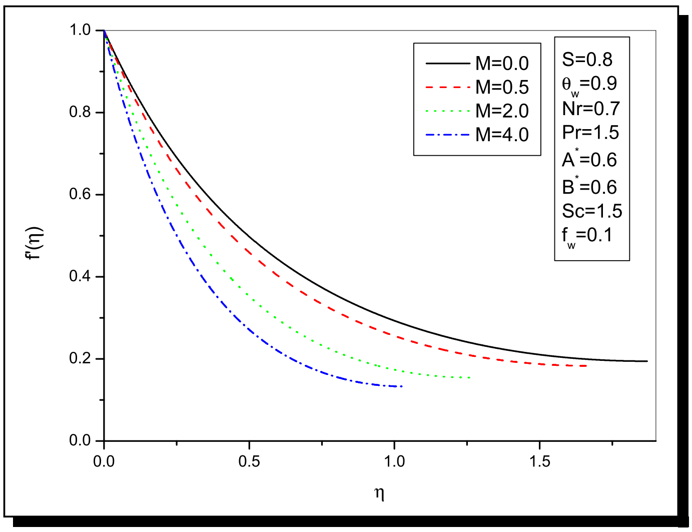

Figure 4. Effects of magnetic parameter M on velocity profile $f'(\eta)$

Figure 4 shows the effect of magnetic parameter M on velocity profile. It is observed from this figure that for increase in the magnetic parameter is to decrease the velocity profile in the thin film. Physically, a drag like force known as Lorentz force is generated for the presence of the transverse magnetic field, which results in decrease the velocity field.

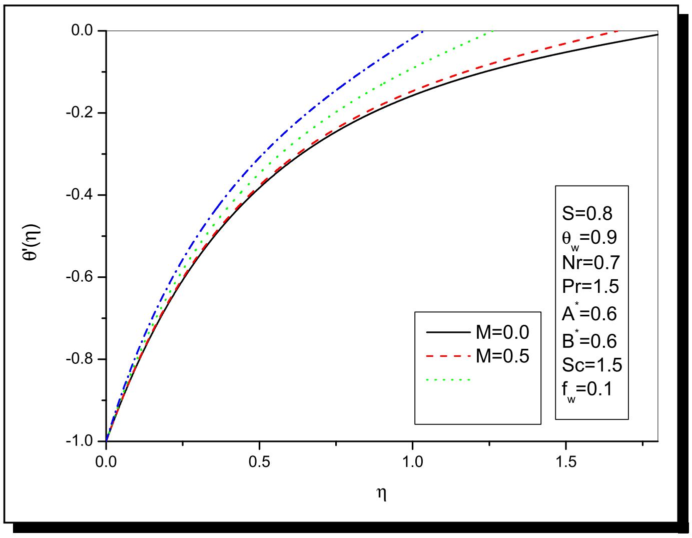

Figure 5. Effects of magnetic parameter M on temperature gradient $\theta'(\eta)$

Figure 5 depicts magnetic parameter effects on the temperature gradient. For the increase of magnetic parameter M then the temperature gradient also increase and thin film thickness η decreases. So transverse magnetic field contributes to the thickening of the thermal boundary layer.

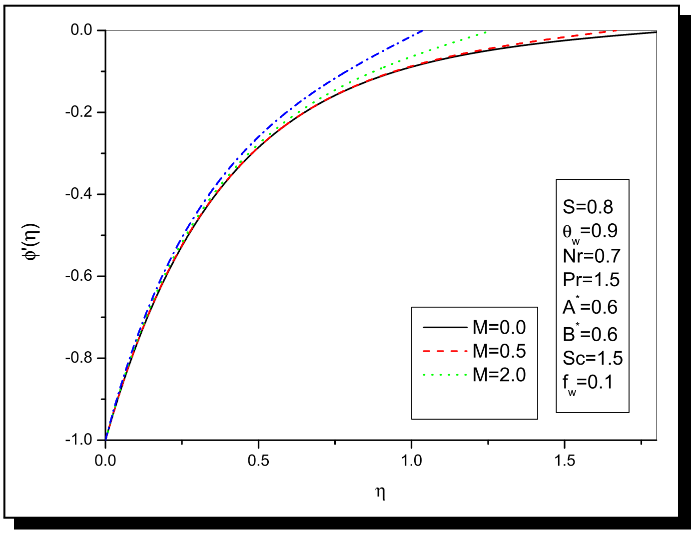

Figure 6. Effects of magnetic parameter M on concentration gradient $\phi'(\eta)$

Figure 6 represents the effect of magnetic parameter M on the concentration gradient. Since a drag force is produce for increasing of the magnetic field which opposes the flow. Thus, as the magnetic parameter M increases there results in increase the concentration gradient.

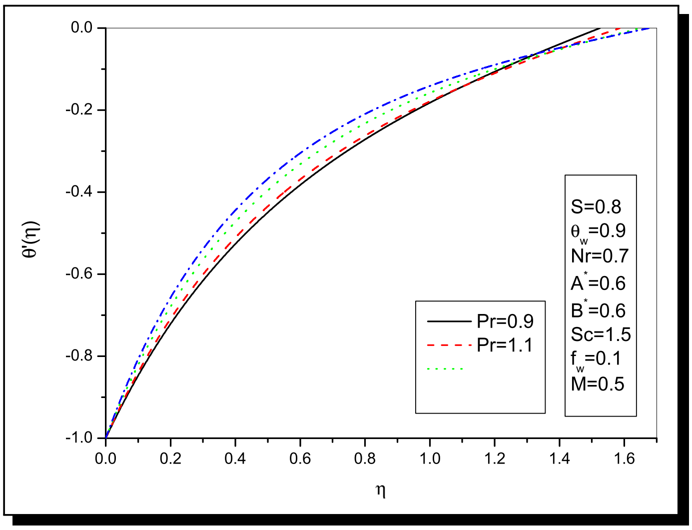

Figure 7. The effect of Prandtl number Pr on temparature gradient $\theta'(\eta)$

Figure 7 shows temperature gradient profile for different values of the Prandtl number. Prandtl number Pr being the ratio of momentum diffusivity and thermal conductivity for a fluid. So for increase of Prandtl number there would be increase in the thin film thickness. Thus, temperature gradient increase for the increase in the values of Prandtl number.

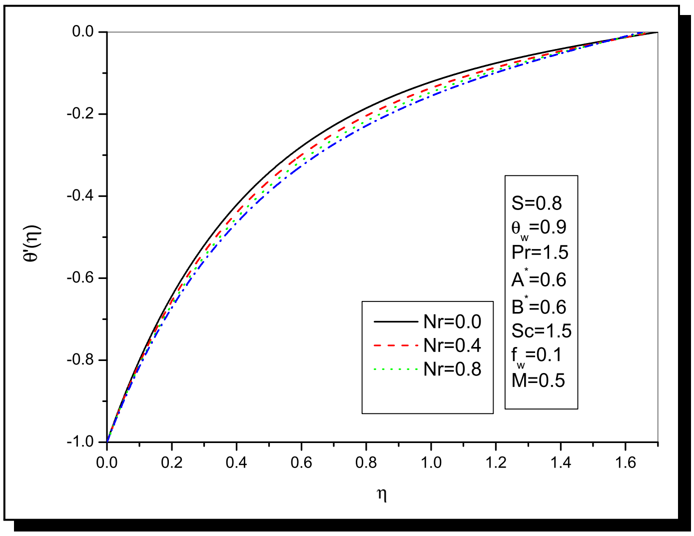

Figure 8. Effect of radiation parametere Nr on temperature gradient $\theta'(\eta)$

Figure 8 shows variation of the temperature gradient along η for different values of thermal radiation parameter Nr. From the expression for $Nr = \frac{16\sigma^* T_0^3}{3k^*\kappa}$, we see that when Nr increases then the Rosseland radiative absorption coefficient k^* decrease, so heat flux q_r $(= -\frac{16\sigma^*}{3k^*} T^3 \frac{\partial T}{\partial y})$ decrease which results temperature gradient decrease. Thus, for increase in the thermal radiation parameter there is decrease in the temperature gradient in the thermal boundary layer.

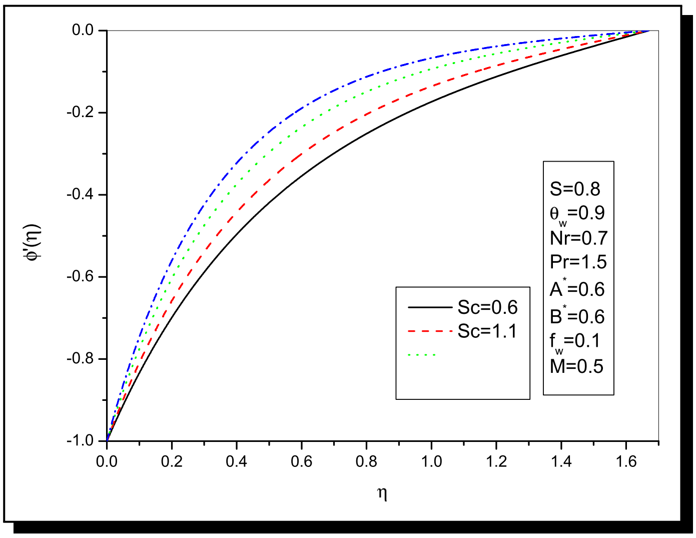

Figure 9. Effects of Scmidth number Sc on concentration gradient $\phi'(\eta)$

Figure 9 shows concentration gradient for different values of Schimdt number Sc. It is observed from this plot that as Schimdt number increases then concentration gradient increases, i.e. mass transfer rate increases. The Schimdt number be the ratio of the momentum to the mass diffusivity and therefore Schmidt number is inversely proportional to the diffusion coefficient D. So, concentration of the fluid decreases with increase of Sc.

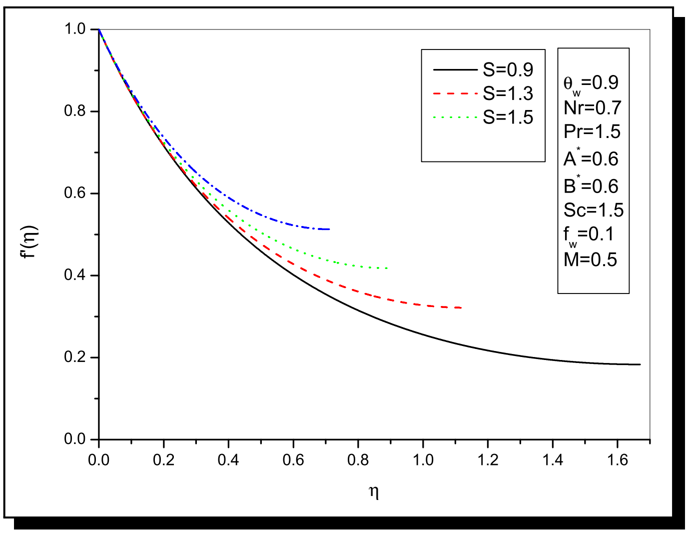

Figure 10. Effects of unsteadiness parameter S on velocity profile $f'(\eta)$

Figure 10 represents the variation of velocity profile for different values of unsteadiness parameter S. It is observed that increase of the unsteadiness parameter S there is increase in the velocity profile of the thin film flow and reduction in the thin film thickness η.

Figure 11 shows that for an increase of unsteadiness parameter S the temperature gradient of the flow increases due to decrease in the thin film thickness η.

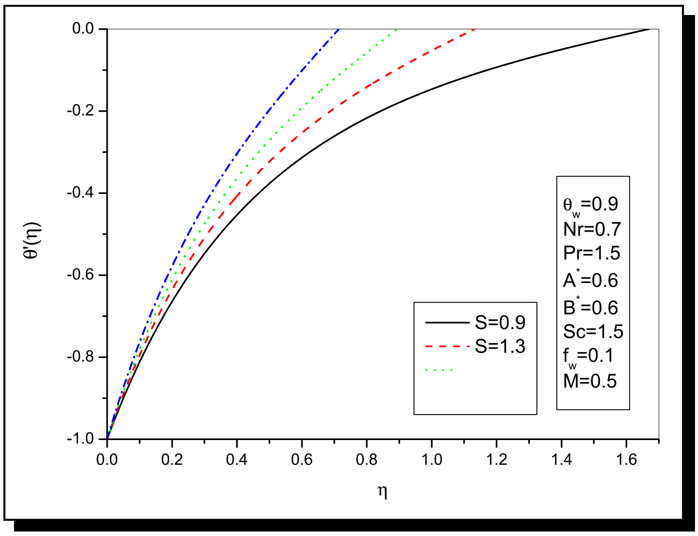

Figure 11. Effects of unsteadiness parameter S on temperature gradient $\theta'(\eta)$

Figure 12 shows that for the increase in the unsteadiness parameter S, the concentration gradient of the flow increases, whereas the thin film thickness η decreases due to which mass transfer rate increases within thin film liquid.

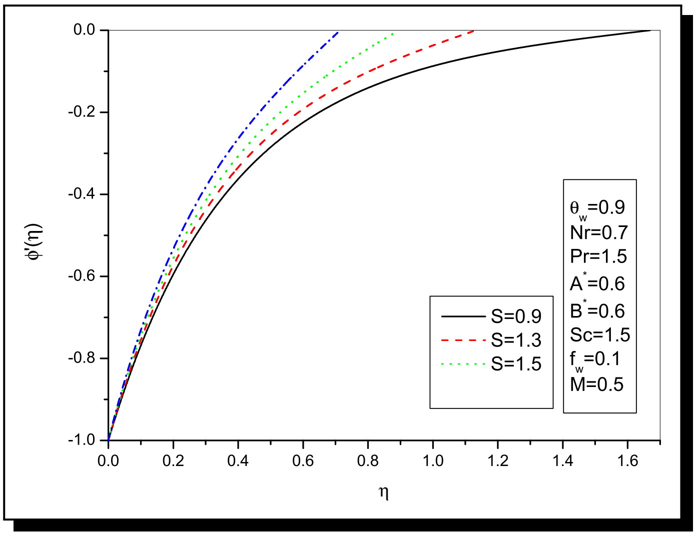

Figure 12. Effects of unsteadiness parameter S on concentration gradient $\phi'(\eta)$

Nomenclature

a,b,d	positive constant
A^*	space dependent heat source-sink parameter
B^*	temperature dependent heat source-sink parameter
B_0	uniform magnetic field
B_1	transverse magnetic field
C	concentration of the fluid

C_p	specific heat at constant pressure
C_{ref}	reference concentration
D	diffusion coefficient
f	dimensionless stream function
f_w	permeability parameter
h	thickness of thin liquid film
k	thermal conductivity
k^*	Rosseland mean spectral absorption coefficient
M	magnetic parameter
Pr	Prandtl number
q	heat flux
q_m	surface mass flux at the stretching surface
q_r	radiative heat flux
q_t	surface heat flux at the stretching surface
Q	heat generation or absorption per unit volume
S	unsteadiness parameter
Sc	Schmidt number
t	time
T	temperature of fluid
T_0	temperature at the slit
T_{ref}	reference temperature
T_s	elastic sheet temperature
u, v	velocity component along x and y direction
U	velocity of stretching sheet
v_w	permeability parameter
x, y	direction along and perpendicular to the plate, respectively

Greek symbols

β	dimensionless thin film thickness
η	similarity variable
μ	viscosity of the fluid
ν	kinematic viscosity of the fluid
ρ	density of the fluid
σ^*	Stefan-Boltzman constant
θ	dimensionless temperature
θ_w	temperature ratio parameter
ϕ	dimensionless concentration

Superscripts

$'$	Differentiation with respect to η

5. Conclusion

The effects of non uniform heat source/sink, thermal radiation, magnetic field is presented. Some of the important findings of the problem are listed below:

(i) Increases of space dependent heat source/sink parameter A^* and temperature dependent heat source/sink parameter B^* temperature gradient is decreases in both cases.

(ii) Thermal radiation decrease the cooling rate of the thin liquid film but reverse effect is seen with the Prandtl number.

(iii) For the increase of the unsteadiness parameter S velocity profile of the thin film flow increase.

(iv) Increasing the magnetic parameter results in decrease in the velocity distribution and increase in the temperature and concentration gradients.

(v) Mass transfer rate increases with increase of the Schimdt number.

Competing Interests

The author declares that he has no competing interests.

Authors' Contributions

The author wrote, read and approved the final manuscript.

References

[1] M.S. Abel, N. Mahesha and J. Tawade, Heat transfer in a liquid film over an unsteady stretching surface with viscous dissipation in presence of external magnetic field, *Applied Mathematical Modelling* **33**(8) (2009), 3430 – 3441, DOI: 10.1016/j.apm.2008.11.021.

[2] M.S. Abel, J. Tawade and M.M. Nandeppanavar, Effect of non-uniform heat source on MHD heat transfer in a liquid film over an unsteady stretching sheet, *International Journal of Non-Linear Mechanics* **44**(9) (2009), 990 – 998, DOI: 10.1016/j.ijnonlinmec.2009.07.004.

[3] R.C. Aziz, I. Hashim and A.K. Alomari, Flow and heat transfer in a liquid film over a permeable stretching sheet, *Journal of Applied Mathematics* **2013** (2013), Article ID 487586, 9 pages, DOI: 10.1155/2013/487586.

[4] L.J. Crane, Flow past a stretching plate, *Zeitschrift für angewandte Mathematik und Physik ZAMP* **21** (1970), 645 – 647, URL: https://link.springer.com/article/10.1007/BF01587695.

[5] M.R. Khan, S. Mao, W. Deebani and A.M.A. Elsiddieg, Numerical analysis of heat transfer and friction drag relating to the effect of Joule heating, viscous dissipation and heat generation/absorption in aligned MHD slip flow of a nanofluid, *International Communications in Heat and Mass Transfer* **131** (2022), 105843, DOI: 10.1016/j.icheatmasstransfer.2021.105843.

[6] F.C. Lai and F.A. Kulacki, The effect of variable viscosity on convective heat transfer along a vertical surface in a saturated porous medium, *International Journal of Heat and Mass Transfer* **33**(5) (1990), 1028 – 1031, DOI: 10.1016/0017-9310(90)90084-8.

[7] I.C. Liu and A.M. Megahed, Homotopy perturbation method for thin film flow and heat transfer over an unsteady stretching sheet with internal heating and variable heat flux, *Journal of Applied Mathematics* **2012** (2012), Article ID 418527, 12 pages, DOI: 10.1155/2012/418527.

[8] I.-C. Liu and A.M. Megahed, Numerical study for the flow and heat transfer in a thin liquid film over an unsteady stretching sheet with variable fluid properties in the presence of thermal radiation, *Journal of Mechanics* **28**(2) (2012), 291 – 297, DOI: 10.1017/jmech.2012.32.

[9] N.F.M. Noor and I. Hashim, Thermocapillarity and magnetic field effects in a thin liquid film on an unsteady stretching surface, *International Journal of Heat and Mass Transfer* **53**(9-10) (2010), 2044 – 2051, DOI: 10.1016/j.ijheatmasstransfer.2009.12.052.

[10] P. Saha, Nonlinear thermal radiation and temperature dependent viscosity effects on MHD heat and mass transfer in a thin liquid film over a stretching surface, *Journal of Mathematical and Computational Science* **11**(6) (2021), 8240 – 8257, DOI: 10.28919/jmcs/6785.

[11] B.C. Sakiadis, Boundary-layer behavior on continuous solid surfaces: I. Boundary-layer equations for two-dimensional and axisymmetric flow, *American Institute of Chemical Engineers Journal* **7**(1) (1961), 26 – 28, DOI: 10.1002/aic.690070108.

[12] M.A. Seddek and A.M. Salem, Further results on the variable viscosity with magnetic field on flow and heat transfer to a continuous moving flat plate, *Physics Letters A* **353**(4) (2006), 337 – 340, DOI: 10.1016/j.physleta.2005.12.095.

[13] R. Tsai, K.H. Huang and J.S. Huang, Flow and heat transfer over an unsteady stretching surface with non-uniform heat source, *International Communications in Heat and Mass Transfer* **35**(10) (2008), 1340 – 1343, DOI: 10.1016/j.icheatmasstransfer.2008.07.001.

[14] K. Vajravelu and D. Rollins, Heat transfer in an electrically conducting fluid over a stretching surface, *International Journal of Non-Linear Mechanics* **27**(2) (1992), 265 – 277, DOI: 10.1016/0020-7462(92)90085-L.

[15] C. Wang, Analytic solutions for a liquid film on an unsteady stretching surface, *Heat and Mass Transfer* **42** (2006), 759 – 766, DOI: 10.1007/s00231-005-0027-0.

[16] J.C. Zhou, A. Abidi, Q.-H. Shi, M.R. Khan, A. Rehman, A. Issakhov and A.M. Galal, Unsteady radiative slip flow of MHD Casson fluid over a permeable stretched surface subject to a non-uniform heat source, *Case Studies in Thermal Engineering* **26** (2021), 101141, DOI: 10.1016/j.csite.2021.101141.